Title

Single Step Isolation and Activation of Primary CD3+ T Lymphocytes Using Alcohol-Dispersed Electrospun Magnetic Nanofibers

Journal

Nano Letters, 12(8)

ISSN

1530-6984

Authors

Kim, Kwanghee
An, Hyo Jin
Jun, Seung-Hyun
et al.

Publication Date

2012-08-08

DOI

10.1021/nl301388d

Peer reviewed

NANO LETTERS

Letter

pubs.acs.org/NanoLett

Single Step Isolation and Activation of Primary CD3$^+$ T Lymphocytes Using Alcohol-Dispersed Electrospun Magnetic Nanofibers

Kwanghee Kim,[†] Hyo Jin An,[‡] Seung-Hyun Jun,[‡] Tae-Jin Kim,[†] Seon Ah Lim,[†] Gayoung Park,[†] Hyon Bin Na,[§] Yong Il Park,[§] Taeghwan Hyeon,[§] Cassian Yee,[∥] Jeffrey A Bluestone,[⊥] Jungbae Kim,*[,‡] and Kyung-Mi Lee*[,†]

[†]Global Research Lab, Department of Biochemistry and Molecular Biology, Korea University College of Medicine, Seoul 136-713, Korea

[‡]Department of Chemical and Biological Engineering, Korea University, Seoul 136-701, Korea

[§]National Creative Research Initiative Center for Oxide Nanocrystalline Materials and School of Chemical and Biological Engineering, Seoul National University, Seoul 151-744, Korea

[∥]Clinical Research Division, Fred Hutchinson Cancer Research Center, Seattle, Washington 98109, United States

[⊥]Diabetes Center and Department of Medicine, University of California, San Francisco, California 94143, United States

Supporting Information

ABSTRACT: Electrospun polymer nanofibers with entrapped magnetic nanoparticles (magnetic NP−NF) represent a novel scaffold substrate that can be functionalized for single-step isolation and activation of specific lymphocyte subsets. Using a surface-embedded T cell receptor ligand/trigger (anti-CD3 monoclonal antibody), we demonstrate, as proof of principle, the use of magnetic NP−NF to specifically isolate, enrich, and activate CD3$^+$ T cells from a heterogeneous cell mixture, leading to preferential expansion of CD8$^+$CD3$^+$ T cells. The large surface area, adjustable antibody density, and embedded paramagnetic properties of the NP−NF permitted enhanced activation and expansion; its use represents a strategy that is amenable to an efficient selection process for adoptive cellular therapy as well as for the isolation of other cellular subsets for downstream translational applications.

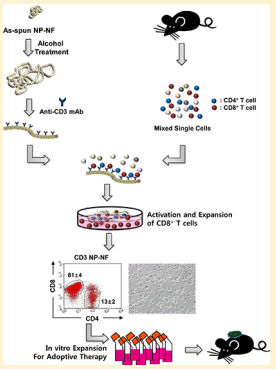

KEYWORDS: *Electrospun magnetic nanofiber, CD4$^+$ T lymphocytes, CD8$^+$ T lymphocytes, anti-CD3 monoclonal antibody, immune cell therapy*

Electrospun nanofibers (NF) are highly versatile reagents exhibiting many favorable design properties such as high surface to volume ratio, durability, ease of handling, and flexibility of forms (as-spun, configured mat, column, etc.).[1−3] These features enable NF to be formulated as tissue engineering scaffolds,[4] biomedical devices,[5] drug delivery carriers,[6] and culture substrate for specialized cell types including mesenchymal stem cells,[7] embryonic stem cells,[8] keratinocytes,[9] and hepatocytes.[10] Among electrospun polymers, polystyrene/poly(styrene-co-maleic anhydride) (PS/PSMA) presents advantages as a NF scaffold substrate due to its inherent ability to cross-link biomolecules. Maleic anhydride groups of PS/PSMA act as molecular anchors allowing covalent attachment of biomolecules to be achieved without further chemical modification.[11−13]

In this study, we exploit these manifold properties to develop a novel application for NF as a single-step isolation and culture platform for T lymphocytes. Since ex vivo enrichment and expansion of tumor-reactive T cells for infusion, known as adoptive cellular therapy, is recognized as a clinically effective modality for the treatment of patients with cancer,[14−16] development of a single-step isolation and culture platform for T lymphocytes would provide significant advances in the technologies of adoptive cellular therapy. To achieve this goal, an idealized solution would be a scaffold that (1) provides a large surface to volume ratio that facilitates cell to surface contact, (2) can be surface-modified for cross-linking of an antibody to a T cell specific marker, (3) allows for rapid and facile separation of bound T cells from mixed population, (4) serves as a depot for selection and stimulation of T cells while enabling its sustained release for downstream applications.

We postulated that PS/PSMA NF would fulfill these criteria when surface modified with anti-CD3 antibody, which serves both as a lymphocyte selection marker and direct T cell activation ligand. Furthermore, entrapping superparamagnetic nanoparticles (NP) to formulate magnetic NP−NF would permit rapid and facile separation of bound CD3$^+$ T cells. Here, we report successful formulation of PS/PSMA NP−NF, surface

Received: April 12, 2012
Revised: July 6, 2012
Published: July 12, 2012

   dx.doi.org/10.1021/nl301388d | *Nano Lett.* 2012, 12, 4018−4024

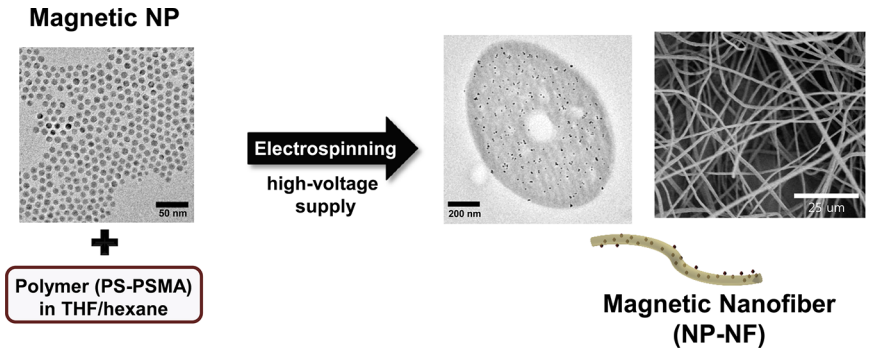

Figure 1. Magnetic NP−NF. Schematic representation for the preparation of magnetic NP−NF is shown. Homogeneous mixtures of PS, PSMA and magnetic NPs at a 2:1:0.023 weight ratio in tetrahydrofuran/hexane were electrospun under a bias of 8−10 kV using a high-voltage supply. The TEM images of 7 nm magnetic NP and as-spun NP−NF are shown. The scale bars in the TEM images of magnetic NP and magnetic NP−NF represent 50 and 200 nm, respectively.

conjugated with anti-CD3 mAb, and its application as a single-step isolation, activation and release platform for $CD3^+$ T lymphocytes.

A schematic describing the preparation of PS/PSMA NF entrapping magnetic NP (magnetic NP−NF) is presented in Figure 1. Magnetic NP synthesized by the thermal decomposition method employing iron oleate-complex[17,18] are uniform in size with an average diameter of 7 nm, as shown in the transmission electron microscope (TEM) image (Figure 1). The homogeneous mixture of PS, PSMA, and magnetic NP at a 2:1:0.023 weight ratio in tetrahydrofuran/hexane was electrospun under a bias of 8−10 kV using a high-voltage supply. A TEM image of microtomed magnetic NP−NF reveals magnetic NP completely embedded and evenly distributed within the polymer nanofibers.[19] Magnetic NP−NFs were then dispersed in 70% ethanol for the purpose of sterilization using methods recently established.[20] EtOH-dispersed NP−NFs could be captured using a conventional magnet within 15 s, enabling easy and rapid recovery from solution (Supporting Information Figure S1A). These magnetic NP−NFs exhibit superparamagnetic properties at room temperature (Supporting Information Figure S1B).

Subsequently, alcohol-dispersed magnetic NP−NF were admixed with anti-CD3 mAb (clone 145−2C11, ebioscience, CA), a T cell receptor (TCR) ligand and trigger for $CD4^+CD3^+$ and $CD8^+CD3^+$ T cells. Clone 145−2C11 was chosen to functionalize NP−NF since its relatively low binding affinity allows $CD3^+$ T cells to be captured and gradually released over time. Anti-CD3 mAb was covalently attached to NP−NF scaffolds (CD3 NP−NF) and subsequently incubated with heterogeneous cell mixtures harvested from various lymph nodes (LN) in mouse (Figure 2A). Both $CD4^+$ and $CD8^+$ T cells bound CD3 NP−NF in approximate proportion to their input frequency (Figure 2A, Supporting Information Figure S3). Fluorescence microscope images demonstrated successful binding of both $CD4^+$ and $CD8^+$ T cells on the CD3 NP−NF scaffolds (Figure 2B). SEM images of magnetic CD3 NP−NF demonstrated binding of T cells on the surface of NF and others deep inside the NF scaffolds (Figure 2C). Neither $CD4^+$ nor $CD8^+$ T cells were bound to NP−NF that were not surface conjugated with anti-CD3 mAb (Supporting Information Figure S3).

When T cell-bound NP−NF scaffold mixtures were put into culture in the presence of stimulating soluble anti-CD3 (clone 145−2C11) and anti-CD28 (clone 37.51) mAbs, bound T cells were gradually released from the NP−NF scaffolds over time (Supporting Information Figure S5). Released cells demonstrated activated "blastlike" appearance to a much higher degree than those positively selected using anti-CD3 mAb-attached magnetic beads (NP) and exposed to soluble anti-CD3 and anti-CD28 (Supporting Information Figure S5). Cells bound onto CD3 NP−NF displayed highly blastoid morphology from day 3 and yielded approximately 8 fold greater cell numbers on day 7 following NP−NF exposure compared with those isolated by CD3 NPs or untreated cells (Figure 3A). Moreover, cells released from CD3 NP−NF expressed higher levels of surface activation markers, CD69, B220, and CD25, than those isolated by CD3 NPs (Figure 3B).

We postulate that this difference in T cell activation between CD3 NP and CD3 NP−NF is attributable to physical characteristics of these structures affecting the presentation of cross-linked anti-CD3 antibodies to the T cells. Because of the small subcellular size of NP (50 nm diameter), anti-CD3 bound to NP (CD3 NP) can only engage a few TCRs at a time. Since many CD3 beads engage TCRs evenly displayed throughout the surface of the T cell, the overall net effect is a weak and diffuse signal of activation. By contrast, when anti-CD3 is bound to larger surfaces such as NP−NF, then many T cell receptors come into contact with the larger area on the anti-CD3 mAb-coated NP−NF scaffold, as shown in Figure 2C. In this case, the CD3 NP−NF scaffold provides a focused, highly polarized and relatively intense signal due to the local concentration of anti-CD3 mAbs, which is critical for TCR cross-linking and downstream intracellular signal amplification leading to T cell activation.[21]

When the proportion of activated $CD4^+$ T versus $CD8^+$ T cells released from CD3 NP−NF was examined, over 77 ± 5% of cells collected from CD3 NP−NF were $CD8^+$ T cells with $CD4^+$ T cells comprising only 16 ± 1% (Figure 4A). Given that the initial pretreatment percentage of $CD4^+$ T cells among $CD3^+$ T cells (56 ± 1%) was higher than that of $CD8^+$ T cells (40 ± 1%) in the input population (Figure 2A), these data would suggest that CD3 NP−NF exposure led to the selective expansion of $CD8^+$ T cells. These results sharply contrast the population of $CD3^+$ T cells cultivated in the absence of NP−NF scaffolds, wherein the percentage of $CD8^+$ T cells at the end of a 6-days culture was only 14 ± 2% and $CD4^+$ T cells, 74 ± 6% (Figure 4A). Cells isolated by NPs via positive selection (CD3 NP) demonstrated an intermediate percentage between the two, comprised of 58 ± 2% $CD8^+$ T cells and 35 ± 3% $CD4^+$ T cells (Figure 4A). Furthermore, $CD8^+$ T cells isolated from CD3 NP−NF demonstrated significantly higher level of

dx.doi.org/10.1021/nl301388d | *Nano Lett.* 2012, 12, 4018−4024

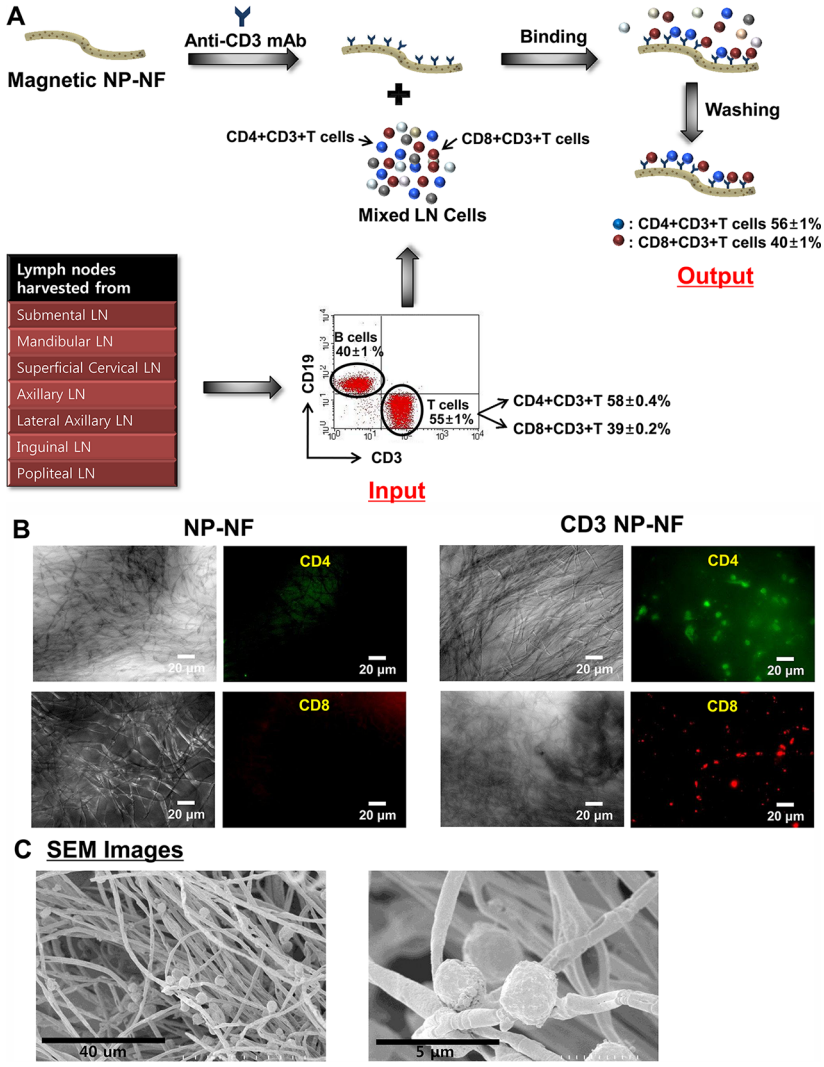

Figure 2. Specific isolation of $CD3^+$ T lymphocytes using magnetic NP−NF. (A) As-spun magnetic NP−NF were dispersed in 70% EtOH and subsequently immobilized with anti-CD3 mAb. Lymph nodes (5×10^6 cells), harvested from C57BL/6 mice, were homogenized to isolate single cells prior to the incubation with magnetic NP−NF conjugated with anti-CD3 mAb (CD3 NP−NF). After 30 min of incubation, the sample was washed and flow cytometry was performed to measure the percentage of $CD4^+$ and $CD8^+$ T cell population among bound $CD3^+$ T cells. Whole LN cells were stained prior to NP−NF treatment and contain approximately, as a percentage of total CD3 T cells, 39 ± 0.2% $CD8^+$ T cells, and 58 ± 0.4% $CD4^+$ T cells which was proportionately similar to the bound T cell subsets (40 ± 1% $CD8^+$ T cells and 56 ± 1% $CD4^+$ T cells). The data shown are representative of five independent experiments, providing the mean values and standard errors of five independent experiments. (B) Shown are pairs of optical (left column) and immunofluorescent (right column) images of $CD4^+$ T cells and $CD8^+$ T cells bound to NP−NF or CD3 NP−NF. NP−NF (left panels) and CD3 NP−NF (right panels) scaffolds stained with FITC-anti-CD4 antibody (green) and PE-anti-CD8 antibody (red), respectively. Cells attached to CD3 NP−NF and NP−NF were visualized by epifluorescence microscopy. These photographs represent one image taken on one *z*-plane of a three-dimensional NP−NF scaffold. While only a few strands of NP−NF appear in focus in the microscope images, there are several dense layers of fibers stacked above and below. These dense regions of NP−NF nonspecifically absorb fluorescent dyes and emit weak, diffuse autofluorescent signals as shown in the NP−NF images. The scale bar in the microscopy images represents 20 μm. (C) Scanning electron microscopy (SEM) images at high magnification (×800 and ×4000) depicting cells bound to CD3 NP−NF. The scale bar in the SEM image represents 40 and 5 μm.

surface CD25 activation marker as compared to those isolated from CD3 NP or nonbound T cell groups (Figure 4B, top panels). In contrast, $CD4^+$ T cells isolated from CD3 NP−NF appeared to have lower levels of CD25 expression than those from CD3 NPs group (Figure 4B, bottom panels), implying that $CD4^+$ T cells found in the CD3 NP−NF group were poorly activated.

The precise mechanism underlying preferential activation and expansion of $CD8^+$ T lymphocytes by CD3 NP−NF is unclear but may be related to the strength of binding between T cells and anti-CD3 mAb conjugated onto solid NP−NF scaffolds. To test this hypothesis, we cultured T cells on solid tissue culture plastic dishes where the strength between TCR/CD3 complex on T cells and anti-CD3 mAb on the plate could be varied by adjusting the concentration of anti-CD3 mAb coated on their surface. Three concentrations of anti-CD3 mAb, 0.1, 0.5, and 1 μg/mL were used representing low, intermediate, and high cross-linking conditions of TCR/CD3 on T cells, respectively (Figure 5). To eliminate the contribution of other cell populations present in whole lymph node extracts in the binding and activation process, especially B lymphocytes, lymph node cells were passed through Nylon

dx.doi.org/10.1021/nl301388d | *Nano Lett.* 2012, 12, 4018−4024

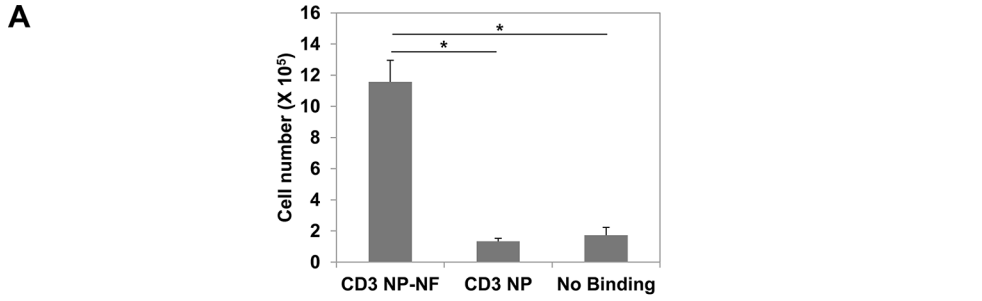

	CD3 NP	CD3 NP-NF
CD69	216±108	456±103*
B220	63±3	166±13*
CD25	11925±3800	26050±3643*

Figure 3. Growth and activation of T cells following exposure to CD3 NP−NF. (A) To evaluate the ability of CD3 NP−NF to activate T cells and stimulate their growth, approximately 5 × 10^5 B cell-depleted lymph node cells were added to wells containing CD3 NP−NF, CD3 NP or "no binding" control well. Each well was supplemented with 1 μg/mL of soluble anti-CD3 mAb and 1 μg/mL of anti-CD28 mAb to stimulate the long-term growth of T cells. The number of cells recovered following 7 days of cultivation is shown. *$p < 0.05$. (B) Surface expression of CD69, B220, and CD25 activation markers on cells obtained as above was assessed by flow cytometry. The histogram data shown are representative of 3 independent experiments with median fluorescence intensity of each marker shown in the table as "median ± S.E." *$p < 0.05$.

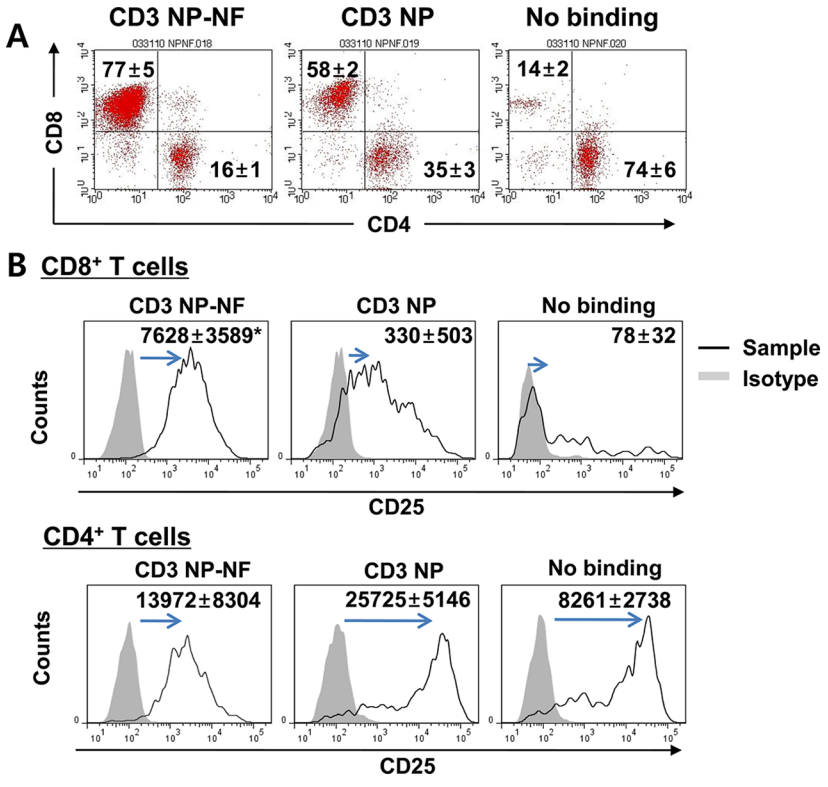

Figure 4. Preferential expansion of $CD8^+$ T cells by NP−NF conjugated with anti-CD3 mAb. (A) Proportion of $CD4^+$ versus $CD8^+$ T cells in the 6 day culture of CD3 NP−NF, CD3 NP, or no-binding group was assessed by flow cytometry and shown as a representative FACS plot. The percentage of $CD4^+$ and $CD8^+$ T cells shown within the FACS plot is the average value among the four experiments and is depicted along with the standard error. (B) Expression of CD25 activation marker was shown on $CD8^+$ T cells (top panels) and $CD4^+$ T (bottom panels) as histograms. The histogram shown is a representative data set for the four independent experiments (median ± S.E). *$p < 0.05$.

dx.doi.org/10.1021/nl301388d | Nano Lett. 2012, 12, 4018−4024

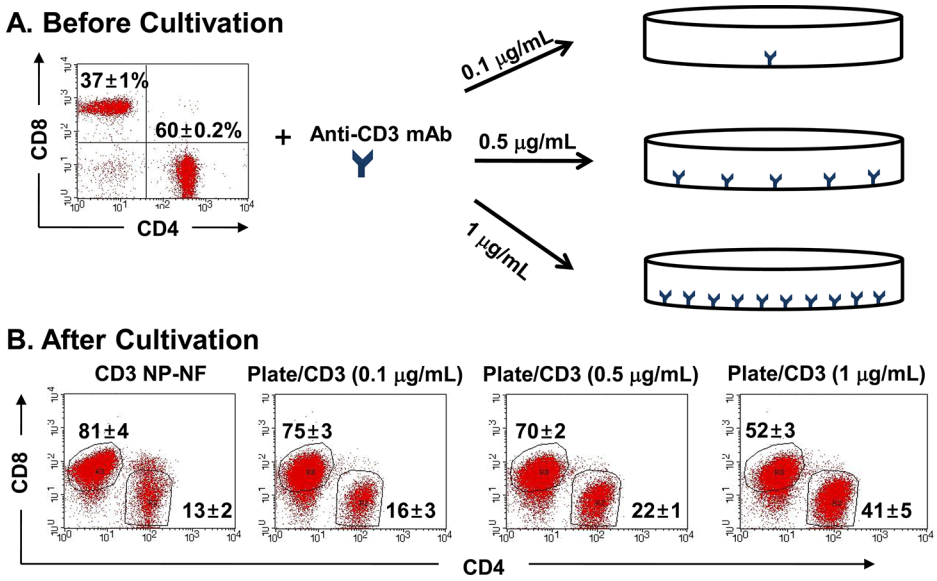

Figure 5. Proportion of $CD4^+$ vs $CD8^+$ T cells cultured on anti-CD3 mAb-coated plates (A) $CD3^+$ T cells were enriched by passing through nylon wool and cultivated on tissue culture plates coated with a low (0.1 μg/mL), intermediate (0.5 μg/mL), or high (1 μg/mL) concentration of anti-CD3 mAb followed by expansion with 1 μg/mL of soluble anti-CD3 mAb and 1 μg/mL of anti-CD28 mAb for 7 days. (B) Harvested cells were analyzed by flow cytometry to determine the percentage of $CD4^+$ and $CD8^+$ T cells.

Wool columns.[22] After passage, initial populations of $CD4^+$ and $CD8^+$ T lymphocytes were 60 ± 0.2% and 37 ± 1%, respectively, as shown in Figure 5A. T cells cultured with the lowest concentration (0.1 μg/mL) of anti-CD3 mAb resulted in the highest percentage of $CD8^+$ T cells (75 ± 3%), a value similar to that obtained when using CD3 NP−NF (Figure 5B). As the concentration of anti-CD3 mAb increased, the percentage of $CD8^+$ T cells decreased; 70 ± 2% and 52 ± 3% at 0.5 and 1 μg/mL, respectively. Taken together, these data suggest that low to intermediate TCR cross-linking with anti-CD3 mAb appeared to drive activation and expansion of $CD8^+$ T cells while strong TCR cross-linking promoted activation of $CD4^+$ T lymphocytes. Therefore, NP−NF facilitated activation and expansion of $CD8^+$ T cells, presumably as a result of low to intermediate TCR cross-linking via anti-CD3 mAb presented by the NP−NF scaffold.

At present, magnetic cell separation is one of the most popular tools for isolating cells of interest.[23,24] Magnetic cell separation utilizes magnetic nanoparticle beads of ~50 nm that are conjugated with monoclonal antibodies generated against cell- or tissue-specific surface receptors to enrich (positively select) or deplete (negatively select) target cells in a heterogeneous cell mixture. Positive selection often yields higher purity of the intended cell population but may cause unexpected cellular effects due to binding of magnetic nanoparticles on cell surface. While cells isolated by negative selection are "untouched" by magnetic nanoparticles, they are often contaminated by the incomplete removal of nontarget cells. Both positive and negative selection also require multiple binding and washing steps to obtain a final enriched cell product and further manipulation in culture wells for in vitro activation.

Our magnetic NP−NF scaffolds offer a significant advance over current approaches in the following aspects: First, one-step isolation of T lymphocytes can be achieved by simple mixing of heterogeneous cell mixtures with anti-CD3 mAb-conjugated NP−NF scaffolds and the whole complex can be transferred for downstream applications in adoptive T cell therapy. Second, the NF scaffolds could function as a reservoir for isolated $CD3^+$ T cells and gradually release them over time. Third, the released and activated $CD3^+$ T cells were mostly $CD8^+CD3^+$ T cells, which are equipped to lyse tumor and virally infected target cells. Fourth, there is minimal or no potential interference in cellular viability or function due to bound beads since magnetic NPs are embedded within NF and do not contact the T cell surface. The hydrophobic capping on the surface of magnetic NP prevents them from leaching out of hydrophobic NF into hydrophilic solution. Finally, NP−NF may be recycled after magnetic retrieval for repeated use.

One important finding from this study was the preferential activation and expansion of $CD8^+$ T cells over $CD4^+$ T cells by CD3 NP−NF scaffolds. The preferential activation of $CD8^+$ T cells using low (0.1 μg/mL), but not intermediate (0.5 μg/mL) or high (1 μg/mL), concentrations of plate-bound anti-CD3 mAb suggests that weak TCR-anti-CD3 mAb interaction under these conditions favor the outgrowth of $CD8^+$ T cells. By contrast, cells isolated by either positive or negative selection using anti-CD3 nanoparticle beads preferentially expand $CD4^+$ T cells, over that of $CD8^+$ T cells, presumably due to strong TCR ligation by anti-CD3 mAb-coated magnetic beads. To our knowledge, this is a novel hypothesis that lower levels of anti-CD3 cross-linking and weaker TCR ligation lead to preferential $CD8^+$ T cell activation. However, these results were not unexpected given the recent reports demonstrating the strong TCR signal requirement for $CD4^+$ T cell differentiation as compared to that for $CD8^+$ T cells in the thymus. Both $CD4^+$ and $CD8^+$ T cells differentiate from $CD4^+CD8^+$ double positive thymocytes during a process called "positive selection". A commonly held perspective is that the strength of TCR signals directs lineage differentiation with stronger and more persistent TCR signals promoting CD4 lineage differentiation while transient signals promoting CD8 lineage differentiation.[25,26] Our observation that $CD8^+$ T cells are preferentially activated by CD3 NP−NF that corresponds to the low-level TCR cross-linking found on anti-CD3 mAb-coated tissue culture plate is consistent with these studies in T cell development and

dx.doi.org/10.1021/nl301388d | Nano Lett. 2012, 12, 4018−4024

provides a rational approach to the use of CD3 NP−NF for adoptive cellular therapy strategies.

The NP−NF scaffold, by incorporating paramagnetic cell capture, enrichment, and activation features in one product, addresses a logistical challenge in immune-based cell therapies. Adoptive cellular therapy, one form of immune-based therapy, involving the isolation and expansion of tumor-reactive T cells, requires extensive in vitro manipulation of lymphocyte subsets to generate a cell product for the treatment of patients with cancer.[16] Current T cell expansion and enrichment approaches require either soluble anti-CD3 in combination with irradiated feeder cells[14] (which serve to cross-link the TCR trigger) or antibody coated beads.[27] In the former, the regulatory constraints associated with the use of allogeneic human cells to expand patient T cells and the infrastructure required to collect and process these cells as well as the availability of a radiation source can be prohibitive for most clinical research centers. In the latter, the use of antibody coated beads involves multiple steps, including pre-expansion removal of phagocytic cells in addition to regulatory concerns related to remnant microbeads in the infused product. The use of embedded magnetic nanoparticles also provides a rapid and convenient in vitro means of separating the NP−NF from unbound cells. The use of an external magnet to separate the NP−NF from the unbound cells while in the mixture vessel requires minimal operator manipulation and is amenable to an automated, large scale and high-throughput process that can be conducted under a closed system enabling its use for clinical applications.

Additionally, we anticipate that the NP−NF platform can be further formulated with biodegradable and biocompatible materials to be applied in vivo. When functionalized with T cell-specific antibodies and bioactive reagents, NP−NF can be loaded with tumor-reactive T cells ex vivo and then implanted in patients near tumor sites or postsurgical sites as adjuvant therapy where the activated T cells can be released in a "depot" manner. The embedded magnetic NP in the NP−NF can then serve a second function by enabling serial imaging with MRI so that clinicians can determine in a noninvasive manner when the NP−NF scaffold has been resorbed/biodegraded and guide decisions related to repeated or alternative therapy.

Several large-scale studies using adoptively transferred tumor-infiltrating lymphocytes (TIL) for patients with metastatic melanoma have demonstrated that clinical efficacy is directly correlated with TIL products in which the predominant population are $CD8^+$ T cells.[15] Anti-CD3 coated NP−NF scaffolds are unique among existing expansion strategies in that it preferentially activates and expands the $CD8^+$ T cell population even when these cells exist in the minority. Therefore, NP−NF scaffolds offer a cost-effective one-step process to acquire highly activated $CD8^+$ T cells in vitro. It is expected that NP−NF scaffolds can also be applied to achieve efficient enrichment, depletion, or activation of a wide variety of cells including various lymphocyte subsets, antigen-presenting cells, tumor cells, or pluripotent stem cells, by identifying a relevant antibody for selection. Furthermore, generation of biodegradable NP−NF allows for direct and sustained delivery to tumor sites not only of T cells bound to NF scaffolds but also other bioactive modalities including DNA vaccines and recombinant plasmids encoding lymphokine genes, i.e., IL-2, IL-12, IL-15, IL-18, and IFN-γ, as a source of T cell growth factors. Thus, the NP−NF scaffold described here offers a readily translatable, cost-effective strategy to efficiently activate and expand specific lymphocyte cell subsets and provides a potential platform for sustained in vivo cell delivery.

■ ASSOCIATED CONTENT

Ⓢ Supporting Information

Experimental details and additional information related to the preparation, physical properties, and function of NP−NF and CD3 NP−NF. This material is available free of charge via the Internet at http://pubs.acs.org.

■ AUTHOR INFORMATION

Corresponding Author

*(K.-M.L.) Tel: +82-2-920-6253. Fax: +82-2-920-6252. E-mail: kyunglee@korea.ac.kr. (J.K.) Tel: +82-2-3290-4850. Fax: +82-2-926-6102. E-mail: jbkim3@korea.ac.kr.

Notes

The authors declare no competing financial interest.

■ ACKNOWLEDGMENTS

This work was supported by the Korea Foundation for International Cooperation of Science, and Technology (KICOS) Grant (K20702001994-11A0500-03610), the Converging Research Center Program (2011K000815), and the National Research Foundation (NRF) Grant (2011K000833) through the Korean Ministry of Education, Science, and Technology.

■ REFERENCES

(1) Bhardwaj, N.; Kundu, S. C. *Biotechnol. Adv.* **2010**, *28* (3), 325−47.
(2) Sell, S. A.; McClure, M. J.; Garg, K.; Wolfe, P. S.; Bowlin, G. L. *Adv. Drug Delivery Rev.* **2009**, *61* (12), 1007−19.
(3) Jang, J. H.; Castano, O.; Kim, H. W. *Adv. Drug Delivery Rev.* **2009**, *61* (12), 1065−1083.
(4) Boudriot, U.; Dersch, R.; Greiner, A.; Wendorff, J. H. *Artif. Organs* **2006**, *30* (10), 785−92.
(5) Huang, C.; Soenen, S. J.; Rejman, J.; Lucas, B.; Braeckmans, K.; Demeester, J.; De Smedt, S. C. *Chem. Soc. Rev.* **2011**, *40* (5), 2417−34.
(6) Yoo, H. S.; Kim, T. G.; Park, T. G. *Adv. Drug Delivery Rev.* **2009**, *61* (12), 1033−42.
(7) Piryaei, A.; Valojerdi, M. R.; Shahsavani, M.; Baharvand, H. *Stem Cell Rev.* **2011**, *7* (1), 103−18.
(8) Xie, J.; Willerth, S. M.; Li, X.; Macewan, M. R.; Rader, A.; Sakiyama-Elbert, S. E.; Xia, Y. *Biomaterials* **2009**, *30* (3), 354−62.
(9) Min, B. M.; Lee, G.; Kim, S. H.; Nam, Y. S.; Lee, T. S.; Park, W. H. *Biomaterials* **2004**, *25* (7−8), 1289−97.
(10) Chua, K. N.; Lim, W. S.; Zhang, P.; Lu, H.; Wen, J.; Ramakrishna, S.; Leong, K. W.; Mao, H. Q. *Biomaterials* **2005**, *26* (15), 2537−47.
(11) Kim, B. C.; Nair, S.; Kim, J.; Kwak, J. H.; Grate, J. W.; Kim, S. H.; Gu, M. B. *Nanotechnology* **2005**, *16* (7), S382−S388.
(12) Nair, S.; Kim, J.; Crawford, B.; Kim, S. H. *Biomacromolecules* **2007**, *8* (4), 1266−1270.
(13) Kim, B. C.; Lopez-Ferrer, D.; Lee, S. M.; Ahn, H. K.; Nair, S.; Kim, S. H.; Kim, B. S.; Petritis, K.; Camp, D. G.; Grate, J. W.; Smith, R. D.; Koo, Y. M.; Gu, M. B.; Kim, J. *Proteomics* **2009**, *9* (7), 1893−900.
(14) Chapuis, A. G.; Thompson, J. A.; Margolin, K. A.; Rodmyre, R.; Lai, I. P.; Dowdy, K.; Farrar, E. A.; Bhatia, S.; Sabath, D. E.; Cao, J.; Li, Y.; Yee, C. *Proc. Natl. Acad. Sci. U.S.A.* **2012**, *109* (12), 4592−7.
(15) Dudley, M. E.; Yang, J. C.; Sherry, R.; Hughes, M. S.; Royal, R.; Kammula, U.; Robbins, P. F.; Huang, J.; Citrin, D. E.; Leitman, S. F.; Wunderlich, J.; Restifo, N. P.; Thomasian, A.; Downey, S. G.; Smith, F. O.; Klapper, J.; Morton, K.; Laurencot, C.; White, D. E.; Rosenberg, S. A. *J. Clin. Oncol.* **2008**, *26* (32), 5233−9.
(16) Stroncek, D. F.; Berger, C.; Cheever, M. A.; Childs, R. W.; Dudley, M. E.; Flynn, P.; Gattinoni, L.; Heath, J. R.; Kalos, M.;

Marincola, F. M.; Miller, J. S.; Mostoslavsky, G.; Powell, D. J., Jr.; Rao, M.; Restifo, N. P.; Rosenberg, S. A.; O'Shea, J.; Melief, C. J. *J. Transl. Med.* **2012**, *10* (1), 48.
(17) Hyeon, T.; Lee, S. S.; Park, J.; Chung, Y.; Bin Na, H. *J. Am. Chem. Soc.* **2001**, *123* (51), 12798−12801.
(18) Park, J.; An, K. J.; Hwang, Y. S.; Park, J. G.; Noh, H. J.; Kim, J. Y.; Park, J. H.; Hwang, N. M.; Hyeon, T. *Nat. Mater.* **2004**, *3* (12), 891−895.
(19) Lee, S. M.; Jin, L. H.; Kim, J. H.; Han, S. O.; Na, H. B.; Hyeon, T.; Koo, Y. M.; Kim, J.; Lee, J. H. *Bioprocess Biosyst. Eng.* **2010**, *33* (1), 141−7.
(20) Jun, S.-H.; Kim, K.; An, H. J.; Kim, B. C.; Sonn, C. H.; Kim, M.; Doh, J.; Yee, C.; Lee, K.-M.; Kim, J. *Adv. Funct. Mater.* **2012**, DOI: 10.1002/adfm.201200657.
(21) Dustin, M. L.; Chakraborty, A. K.; Shaw, A. S. *Cold Spring Harbor Perspect. Biol.* **2010**, *2* (10), a002311.
(22) Julius, M. H.; Simpson, E.; Herzenberg, L. A. *Eur. J. Immunol.* **1973**, *3* (10), 645−9.
(23) McCloskey, K. E.; Chalmers, J. J.; Zborowski, M. *Anal. Chem.* **2003**, *75* (24), 6868−6874.
(24) Yoon, T. J.; Yu, K. N.; Kim, E.; Kim, J. S.; Kim, B. G.; Yun, S. H.; Sohn, B. H.; Cho, M. H.; Lee, J. K.; Park, S. B. *Small* **2006**, *2* (2), 209−215.
(25) Yasutomo, K.; Doyle, C.; Miele, L.; Fuchs, C.; Germain, R. N. *Nature* **2000**, *404* (6777), 506−10.
(26) Liu, X.; Bosselut, R. *Nat. Immunol.* **2004**, *5* (3), 280−8.
(27) Rasmussen, A. M.; Borelli, G.; Hoel, H. J.; Lislerud, K.; Gaudernack, G.; Kvalheim, G.; Aarvak, T. *J. Immunol. Methods* **2010**, *355* (1−2), 52−60.